Characterization and modeling of the temperature effect on the piezoelectric tube actuator

Didace Habineza, Mahmoud Zouari, Mounir Hammouche, Yann Le Gorrec and Micky Rakotondrabe

* *The authors are with FEMTO-ST Institute, AS2M department, Université Bourgogne Franche-Comté, Université de Franche-Comté/CNRS/ENSMM, 24 rue Savary, 25000 Besançon, France. (e-mail: didace.habineza@femto-st.fr).*

Abstract: This paper deals with the characterization and the modeling of the temperature effect on the piezoelectric tube actuator. Besides the sensitivity to the variation of the temperature, this actuator is characterized by the hysteresis and the creep non-linearities, the badly-damped vibration and the cross-couplings between its three axis. First, the characterization results of the sensitivity of this actuator to the temperature variation (thermo-mechanical deflection) are presented. Then, the effect of the temperature on the hysteresis, the creep, the vibration and the cross-couplings is presented. Finally, from the existing electro-mechanical model of the deflection of the piezoelectric actuators, the temperature-dependent model is proposed. The validation results on one of the piezoelectric tube axis demonstrates the efficacy of the proposed modeling approach.

Keywords: Characterization, modeling, temperature effect, hysteresis, creep, vibration, piezoelectric tube.

1. INTRODUCTION

Piezoelectric actuators are very known in various applications at micro/nano-scale. These applications include nano/micro-positioning (1; 2; 3), -manipulation (4; 5), -assembly (6; 7; 8), etc. The popularity of these actuators is mainly due to the good performances that they offer: the nanometric resolution, the high resolution (more than 1kHz possible), the facility of alimentation and integration in microsystems, etc. From a functional point of view, piezoelectric actuators can be categorized into two groups. The first group includes mono-axis piezoelectric actuators, designed to provide deflections along one direction (e.g. the unimorph cantilevers and piezostacks). Mono-axis piezoelectric actuators are used mainly for manipulation and assembly tasks. The second group concerns the multi-axis piezoelectric actuators, designed to bend along different directions (e.g. the piezoelectric tube called also piezotube). Multi-axis actuators are mainly used for spatial positioning tasks, such as scanning probe microscopy (9).

Despite these advantages, piezoelectric actuators exhibit the hysteresis and the creep nonlinearities, the badly-damped vibration due to their cantilevered structure and the cross-coupling effect for multi-axis actuators such as the piezotube. In addition to the aforementioned drawbacks, piezoelectric material are very sensitive to the variation of the temperature. Consequently, the good working performances of the piezoelectric actuators are compromised when they are working in a temperature varying environment.

The characterization, the modeling and the control of the hysteresis, the creep and the badly-damped vibration have been widely studied, for mono-axis (10; 11; 12; 13) and for multi-axis (14; 15; 16; 17) piezoelectric actuators. However, the issue of the temperature effect is still to be established.

In (18), the effect of the temperature effect on a piezoelectric stack is studied but the study is limited to its impact on the hysteresis. In (19), the temperature effect on the hysteresis, the creep and the vibration was characterized but not modelled. In addition, the characterization in the aforementioned works concerned the case of mono-axis actuators and the issue of the cross-coupling effect has not been addressed. In (20; 21; 22), the impact of the temperature variation on the piezoelectric coefficients has been evaluated. The modeling strategy based on this study leads to physical models of the piezoelectric actuators. The physical models permit to have more information about the actuator. However, they represent a high degree of parametrization, which leads to complex identification and difficult extension to multivariable modeling.

In this paper, we characterize the temperature effect on the piezotube. In addition to the hysteresis, the creep and the vibration, the effect of temperature on cross-couplings is also evaluated. The characterization process is performed inside a dedicated temperature controlled room. To model

* This work is supported by the national ANR-JCJC C-MUMS-project (National young investigator project ANR-12-JS03007.01: Control of Multivariable Piezoelectric Microsystems with Minimization of Sensors). This work has also been supported by the Labex ACTION project (contract "ANR-11-LABX-01-01").

the temperature effect we use the phenomenological model (input-output or black box model) of the deflection of a piezoelectric actuator. Contrary to the physical models, the phenomenological models have the advantage of being simple and easy to identify. First, we propose the mono-variable temperature-dependent model which includes the thermo-mechanical effect, the hysteresis, the creep and the vibration. Then, after its identification and validation, its extension to the multivariable modeling is proposed. The proposed multivariable model is adapted to systems with the same number of inputs and outputs (fully actuated systems) but also to the systems with a different number of inputs and outputs (under or over actuated systems).

This paper is organized as follows. Section II presents the piezoelectric tube, its working principle and the experimental setup. In section III, we present the experimental procedure, the characterization results and discussions. Section IV is devoted to the modeling of the temperature effect. Finally, conclusions and perspectives are drawn in section V.

2. PRESENTATION OF THE PIEZOELECTRIC TUBE AND EXPERIMENTAL SETUP

2.1 Presentation of the piezoelectric tube and its working principle

The actuator used for experimentations in this paper is the PT 230.94 piezoelectric tube (called also piezotube), fabricated by *Physik Instrumente* company. Its presentation and working principle are described in Fig. 1. It is made of the PZT material coated by four external electrodes +x, -x, +y and -y, and one inner electrode (Fig. 1a). Voltages U_x and U_x (U_y and U_y) can be applied on +x and -x (+y and -y) electrodes in order to bend the tube along X-axis (along Y-axis). To obtain the elongation of the tube along Z-axis, the same voltage U_z is applied simultaneously on the four external electrodes (Fig. 1b).

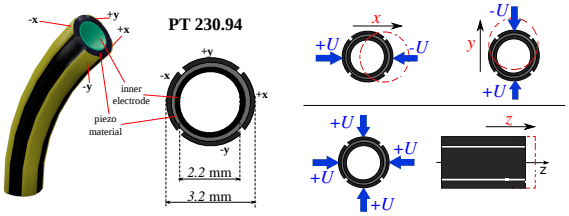

Fig. 1. Description and working principle of the piezoelectric tube. (a) Perspective and top views of the tube, (b) Working principle: application of voltages U and $-U$ in order to get deflections along X, Y and Z axis.

Hence, from the modeling point of view, the piezoelectric tube corresponds to a multivariable system, with three inputs (voltages U_x, U_y and U_z) and three outputs (deflections x, y and z).

2.2 Experimental setup

The experimental setup (Fig. 2) is composed of a piezoelectric tube, a computer with *Matlab/Simulink* software, three optical displacement sensors and voltage amplifiers. The optical sensors and the piezotube are enclosed inside a dedicated temperature controlled room. This room has a specific temperature measurement system, allowing to record the evolution of the temperature inside the room.

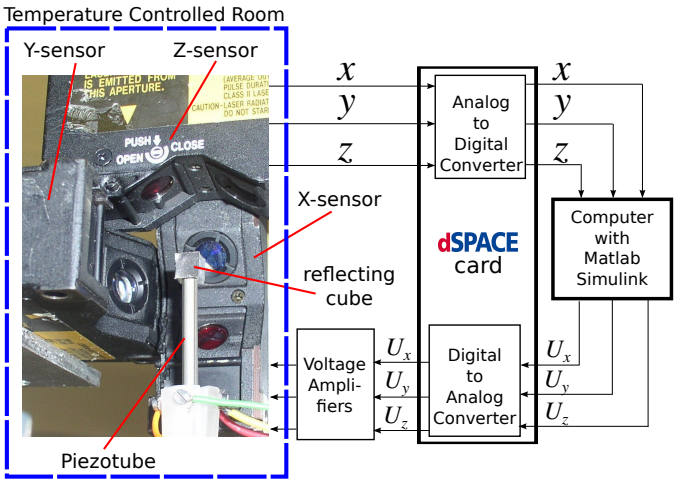

Fig. 2. The description of the experimental setup.

Both displacement sensors and voltage amplifiers are connected to the computer through a dSPACE-1103 board. The operating voltage range of the PT230.94 is ±250V for a deflection of 35μm. Hence, two voltage amplifiers are used to amplify the dSPACE board output voltages, for which the maximum range is about 10V . The tube deflections are measured by using the LC-2420 displacement sensors (fabricated by *Keyence* company). A small cube with perpendicular and flat sides is placed on the top of the tube to allow a linear displacement measurement by optical sensors (which is not possible with the tubular shape of the piezotube). The LC-2420 sensors have 10nm resolution, a bandwidth of 50kHz with a working temperature range between 0 and 40°C.

3. CHARACTERIZATION OF THE TEMPERATURE EFFECT

3.1 Characterization procedure

The characterization has been carried out for the temperature range between 23°C to 39°C, with an increment of 0.5°C, i.e $T_{i+1} = T_i + 0.5$ with T_0=23°C.

For each T_i, the following effects are characterized:

- the sensitivity of the actuator to the variation of the temperature (the thermo-mechanical deflection);
- the hysteresis, the creep and the badly-damped vibration.

3.2 Thermo-mechanical deflection

The evaluation of the thermo-mechanical deflection is performed as follows. After taking all the required characterizations at T_i, the voltage applied to the actuator is put to zero and the position of the tip of the actuator y_{T_i} is recorded. Then, the temperature is increased from T_i to T_{i+1}. When the temperature reaches T_{i+1} the position

of the tip ($y_{T_{i+1}}$) is recorded again and compared to y_{T_i}. This comparison gives the sensitivity of the actuator to the variation of the temperature from T_i to T_{i+1}. The evaluation of this variation along the entire temperature characterization range gives the sensitivity of the actuator to the temperature (the thermo-mechanical deflection). This thermo-mechanical deflection for axis X, Y and Z is represented in Fig 3.

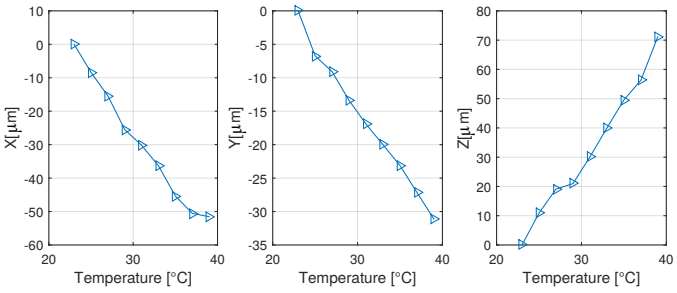

Fig. 3. The characterization of the thermo-mechanical deflection: sensitivity of the actuator to the variation of the temperature.

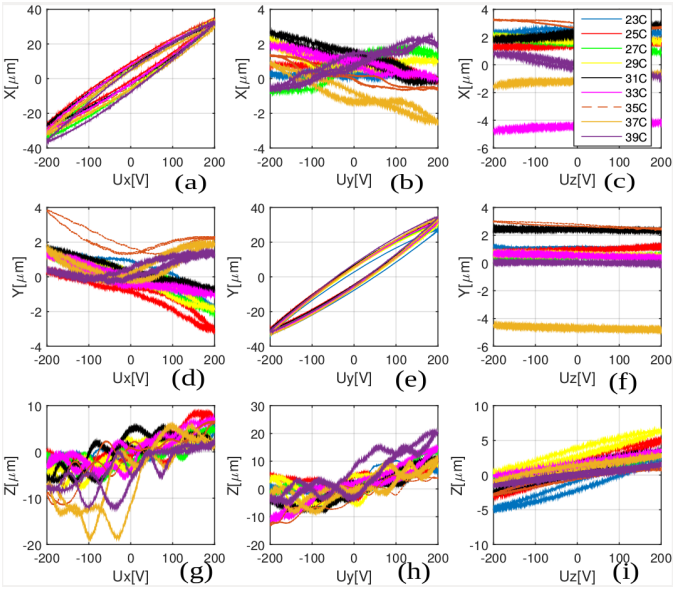

Fig. 4. The characterization of the effect of the temperature on the hysteresis.

It is noticed that the piezoelectric actuator is very sensitive to the variation of the temperature. Considering a linear approximation, the slopes of the sensitivity curves are: 3.8μm/°C for X axis, 2.0μm/°C for Y axis and 4.3μm/°C for Z axis.

3.3 Hysteresis

The hysteresis is characterized as follows. First, a sine voltage $U_x = U\sin(2\pi ft)$ with $U = 200$V and $f = 0.1$Hz is applied on +x and -x electrodes of the piezotube (see Fig. 1b) while U_y and U_z are set to zero. Therefore, the deflection along X axis is observed but also residual deflections along Y and Z axis. The deflection x with respect to the applied U_x (the direct hysteresis) is represented in Fig. 4a and deflections y and z with respect to U_x (coupling hysteresis) are represented in Fig. 4d and Fig. 4g, respectively. To capture the rest of the hysteresis curves, the same procedure is repeated for U_y and U_z.

To characterize the effect of the temperature on the hysteresis, the procedure detailed above is effectuated for each T_i. The characterisation results are gathered in Fig. 4.

It is noticed that the temperature variation impacts hysteresis in direct transfers and in cross-couplings. The hysteresis curves shapes do not change considerably but we notice the change in inclination of hysteresis curves as the temperature changes.

3.4 Vibration

The badly-damped vibrations are characterized by following the same steps as the characterization of hysteresis but instead using of a sine input, a step input of 200V is used. These vibrations correspond to the transient part of the step response. Hence, they are recorded during the short amount of time (15ms in this paper) following the application of the step voltage. The obtained characterizations for each temperature T_i are represented in Fig. 5. Note that the deflections in this figure correspond to the electro-mechanical deflection of the actuator. The thermo-mechanical part has been removed before the presentation.

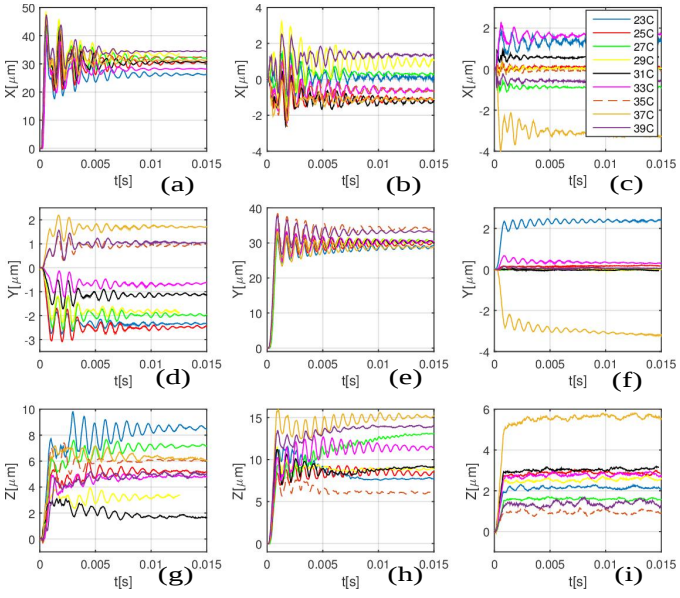

Fig. 5. The characterization of the effect of the temperature on the vibration.

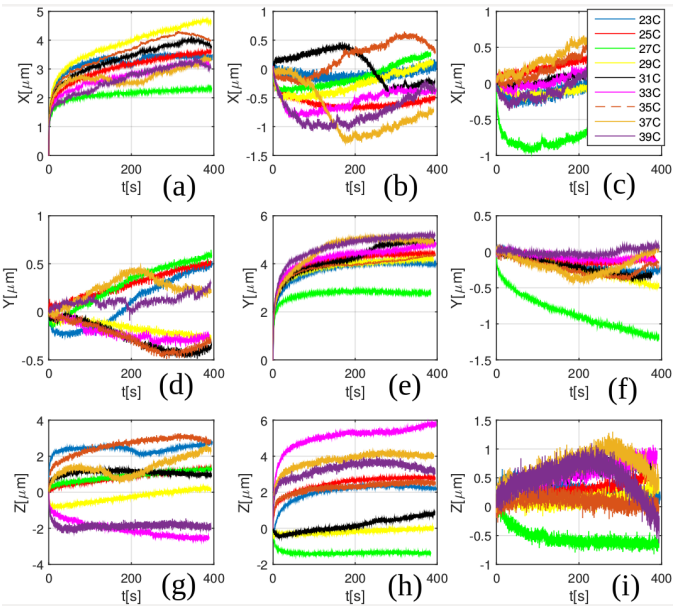

Fig. 6. The characterization of the effect of the temperature on the creep.

It is noticed that the actuator dynamics change with the temperature, for the direct transfers and for the cross-couplings. In addition, we can approximate the electro-mechanical gain of the piezotube for X, Y and Z axis. Considering the direct transfers in Fig. 5a,e and i, it is seen that the application of a step of 200V corresponds to a deflection of 30μm for X and Y axis and 2.5μm for Z axis. This corresponds to an approximative electro-mechanical gain of 0.150μm/V for X and Y axis, and 0.012μm/V for Z axis. These gains are about 20 times smaller than the thermo-mechanical transfer gains identified in section III-B.

3.5 Creep

The creep is identified by following the same steps as the vibration. However, the creep effect is observed on a relatively long period of time compared to the vibration. In this characterization process, a time of 400s has been used. The characterized creep curves are represented in Fig. 6. Note that these curves correspond to the tube deflection after the transient part of a step response.

It is noticed that the amount of creep changes with the temperature, for the direct transfers and the creep.

4. MODELING OF THE TEMPERATURE EFFECT

4.1 General model of the piezoelectric actuator deflection

As stated in Introduction, we use the input-output model, relating the applied voltage U and the deflection of the actuator y, as represented in Fig. 7.

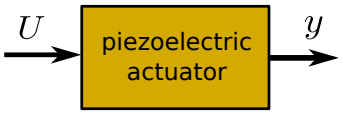

Fig. 7. The input-output modeling scheme of a piezoelectric actuator, relating the input voltage and the output deflection of the actuator.

To relate U and y we have used the existing model of the deflection of a piezoelectric actuator, validated and used in (23; 24) to model the deflection of a mono-axis piezoelectric cantilever. This model is represented by Eq. 1.

$$y(s) = \underbrace{D(s)}_{\text{dynamics}} \underbrace{\Gamma_U(U,s)}_{\text{hysteresis}} + \underbrace{Cr(s)\,U(s)}_{\text{creep}}. \qquad (1)$$

In this equation, $U(s)$ and $y(s)$ represent the Laplace transform of the voltage U and the deflection y. $D(s)$ and $Cr(s)$ represent the LTI models of the dynamics and the creep, respectively. The operator $\Gamma_U(U,s)$ models the hysteresis nonlinearity.

There exist a large number of mathematical models for hysteresis in the literature. To model hysteresis of piezoelectric actuators the most used approaches are Preisach

(25), Prandtl-Ishlinskii (26; 27) and Bouc-Wen (28; 29). The Bouc-Wen approach presents the advantage of using a limited number of parameters and being easy to identify, compared to the other approaches. The Classical Bouc-Wen model is represented by Eq. 2

$$\begin{cases} \Gamma_U(U,s) = d_p U(s) - h(s) \\ \dot{h}(t) = A\dot{U}(t) - \beta|\dot{U}(t)|h(t) - \gamma\dot{U}(t)|h(t)| \end{cases}, \quad (2)$$

where d_p, A, β and γ are the model parameters, which are positive or negative real numbers. $h(s)$ is the Laplace transform of the internal variable of hysteresis $h(t)$, defined by the second equation of Eq. 2.

By combining Eq. 1 and Eq. 2, we find the complete model of the deflection y, due to the application of the voltage U:

$$\begin{cases} y(s) = D(s)\left[d_p U(s) - h(s)\right] + Cr(s)U(s) \\ \dot{h}(t) = A\dot{U}(t) - \beta|\dot{U}(t)|h(t) - \gamma\dot{U}(t)|h(t)| \end{cases}. \quad (3)$$

4.2 The monovariable temperature-dependent model

Considering the variation of the temperature, the complete deflection of the actuator is composed of two deflections: the electro-mechanical deflection y_U defined by Eq. 3 and the thermo-mechanical deflection y_T, defined by

$$y_T = \Gamma_T(T), \quad (4)$$

with Γ_T the thermo-mechanical operator.

Assuming that these two deflections are additive, the entire actuator deflection is defined as:

$$y = y_T + y_U. \quad (5)$$

From Eq. 3, Eq. 4 and Eq. 5, the temperature-dependent model of the piezoelectric actuator is defined as

$$\begin{cases} y(s) = \Gamma_T(T) + D(s,T)\left[d_p(T)U(s) - h(s)\right] \\ \qquad +Cr(s,T)U(s) \\ \dot{h}(t) = A(T)\dot{U}(t) - \beta(T)|\dot{U}(t)|h(t) - \gamma(T)\dot{U}(t)|h(t)| \end{cases}. \quad (6)$$

This model can be implemented as in Fig. 8

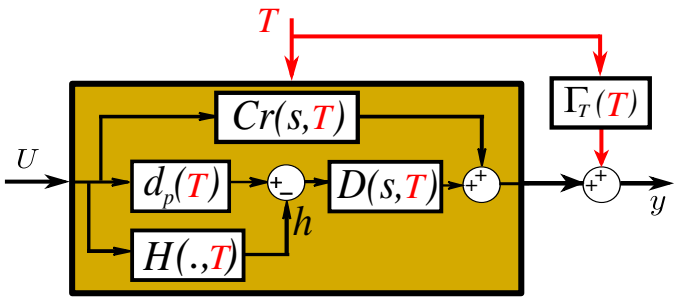

Fig. 8. Implementation scheme of the temperature-dependent model.

4.3 Identification of the monovariable temperature-dependent model

The identification and the validation has been performed for the data from the characterization of X axis of the piezotube (the data represented in Fig. 3a, Fig. 4a, Fig. 5a and Fig. 6a).

From the model of Eq. 6, the parameters to be identified are:

- **The thermo-mechanical operator** $\Gamma_T(T)$: this operator is identified by applying the polynomial interpolation on the data represented in Fig. 3a. By assuming a linear interpolation, the polynomial $\Gamma_T(T) = -3.8T + 82.1$ is obtained.
- **The temperature-dependent LTI model of dynamics** $D(s,T)$: the dynamic part is estimated by applying the function *ident* of *Matlab Identification Toolbox* (30) on the step responses of Fig. 5a. The obtained transfer functions are under the form:

$$G(s) = \frac{b_7 s^7 + \cdots + b_1 s + b_0}{a_8 s^8 + a_7 s^7 + \cdots + a_1 s + a_0}, \quad (7)$$

with b_i $(0 \leq i \leq 7)$ the coefficients of the numerator, and a_i $(0 \leq i \leq 8)$ the coefficients of the denominator. Afterwards, the transfer functions $G(s)$ are normalized and put under the form:

$$D(s) = \frac{n_7 s^7 + \cdots + n_1 s + n_0}{d_8 s^8 + d_7 s^7 + \cdots + d_1 s + d_0}, \quad (8)$$

with $D(s=0) = 1$ (i.e $n_0 = d_0$). By considering all the normalized transfer functions $D(s)$ identified for each temperature T_i, we interpolate the polynomial coefficients $n_i(T)$ and $d_i(T)$, and therefore the temperature-dependent dynamic $D(s,T)$:

$$D(s,T) = \frac{n_7(T)s^7 + \cdots + n_1(T)s + n_0(T)}{d_8(T)s^8 + d_7(T)s^7 + \cdots + d_1(T)s + d_0(T)}. \quad (9)$$

- **The temperature-dependent LTI model of the creep** $Cr(s,T)$: the creep LTI model is obtained by following the same procedure as the estimation of $G(s)$ (by applying the *Matlab Identification Toolbox*) on the data of Fig. 6a. For each temperature, the obtained model is of the form:

$$Cr(s) = \frac{n_2 s^2 + n_1 s + n_0}{d_2 s^2 + d_1 s + d_0}. \quad (10)$$

By identifying $Cr(s)$ for each temperature, the coefficients n_i and d_i are obtained. These coefficients are interpolated in order to find the polynomial coefficients $n_i(T)$ and $d_i(T)$. Finally, the temperature-dependent model of the creep is obtained:

$$Cr(s,T) = \frac{n_2(T)s^2 + n_1(T)s + n_0(T)}{d_2(T)s^2 + d_1(T)s + d_0(T)}. \quad (11)$$

- **The temperature-dependent parameters of the Classical Bouc-Wen model** $d_p(T)$, $A(T)$, $\beta(T)$, and $\gamma(T)$: these parameters are identified from the hysteresis curves of Fig. 4a. First, the Least Square Method is applied to each hysteresis curve in order to find the Bouc-Wen parameters for each temperature.

Then, the obtained parameters are interpolated in order to find the temperature-dependent Bouc-Wen parameters $d_p(T)$, $A(T)$, $\beta(T)$, and $\gamma(T)$.

4.4 Validation of the monovariable temperature-dependent model

After finding the polynomials $\Gamma_T(T)$, $d_p(T)$, $A(T)$, $\beta(T)$, $\gamma(T)$, and the polynomial coefficients of the functions $D(s,T)$ and $Cr(s,T)$, the model of Eq. 6 has been implemented in *Matlab/Simulink* according to the scheme of Fig. 8. Then, the simulation and the experimental data have been compared.

Fig. 9, Fig. 10 and Fig. 11 represent this comparison for the hysteresis, the creep and the vibration, respectively. Note that the temperatures 28.5°C, 32.5°C and 33°C used for the validation have not been taken into account during the parameters interpolation procedure.

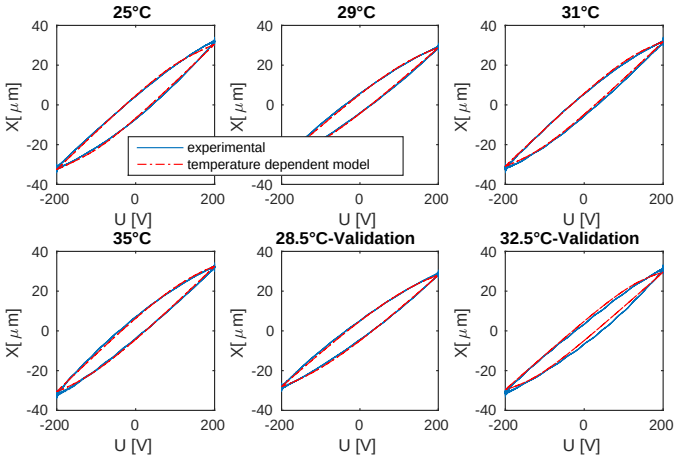

Fig. 9. Validation of the hysteresis.

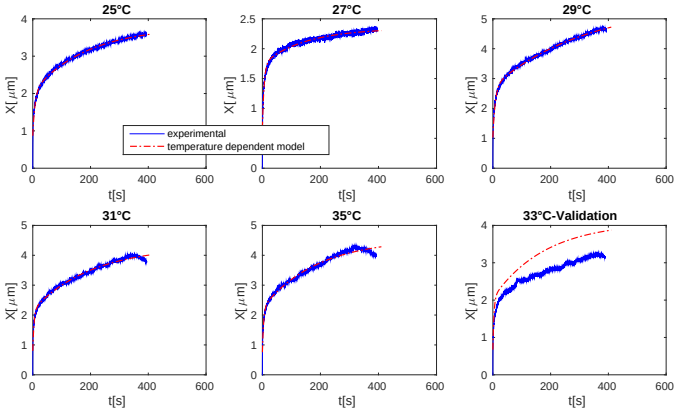

Fig. 10. Validation of the creep.

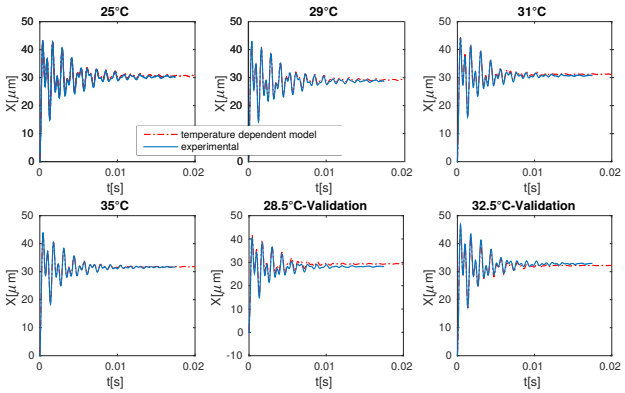

Fig. 11. Validation of the hysteresis.

It is noticed that the proposed model is close to the characterization data even for the temperatures in the characterization range but not taken into account during the interpolation.

4.5 Extension to multivariable temperature-dependent model

The model of Eq. 6 is adapted to systems with one input and one output. Consider now a system with k inputs and n outputs. U and y become then the vectors of k voltages and n deflections, respectively. The multivariable model relating U and y is:

$$\begin{cases} y = \Gamma_T(T) + \hat{D}(s,T)\left[\hat{D}_p(T)U - \hat{h}\right] + Cr(s,T)U \\ \dot{h} = A(T)\dot{U} - \hat{B}(T)\left(|\dot{\hat{U}}| \circ \hat{h}\right) - \hat{\Gamma}(T)\left(\dot{\hat{U}} \circ |\hat{h}|\right) \end{cases}, \tag{12}$$

with $U = (U_1, U_2, \cdots, U_k)^T$, $y = (y_1, y_2, \cdots, y_n)^T$ and $h = (h_1, h_2, \cdots, h_n)^T$. The operation $\circ$ denotes the Hadamard product of matrices. $\Gamma_T(T)$ is the vector of thermo-mechanical operators ($\Gamma_T = (\Gamma_{T1}, \Gamma_{T2}, \cdots, \Gamma_{Tn})^T$). $D(s,T)$ and $Cr(s,T)$ are the matrices of the temperature-dependent LTI models of the vibration and the creep, respectively. $D_p(T)$, $A(T)$, $B(T)$ and $\Gamma(T)$ are the temperature-dependent Bouc-Wen matrices.

Matrices $\hat{D}$, $\hat{D}_p$, $\hat{h}$, $\hat{B}$, $\hat{U}$ and $\hat{\Gamma}$ are defined from D, D_p, h, B, U and Γ as follows:

$$\begin{cases} \text{if } n > k, & \hat{D} = \left[D; \mathbb{O}_{n\times(n-k)}\right],\ \hat{D}_p = D_p, \\ & \hat{B} = \left[B; \mathbb{O}_{n\times(n-k)}\right],\ \hat{\Gamma} = \left[\Gamma; \mathbb{O}_{n\times(n-k)}\right], \\ & \dot{\hat{U}} = \left[\dot{U}; \mathbb{O}_{(n-k)\times 1}\right] \text{ and } \hat{h} = h; \\ \text{if } n < k, & \hat{D} = D,\ \hat{D}_p = \left[D_p; \mathbb{O}_{(k-n)\times k}\right], \\ & \hat{B} = B,\ \hat{\Gamma} = \Gamma, \\ & \dot{\hat{U}} = \dot{U} \text{ and } \hat{h} = \left[h; \mathbb{O}_{(k-n)\times 1}\right]; \\ \text{if } n = k, & \hat{D} = D,\ \hat{D}_p = D_p,\ \dot{\hat{U}} = \dot{U} \text{ and } \hat{h} = h, \end{cases} \tag{13}$$

where $\mathbb{O}_{n\times k}$ is a matrix of zeros with n lines and k columns. For example, considering a system with one input and two outputs ($n = 2$ and $k = 1$), the multivariable temperature-dependent model is:

$$\begin{cases} \begin{pmatrix} y_1 \\ y_2 \end{pmatrix} = \begin{pmatrix} \Gamma_{T1} \\ \Gamma_{T2} \end{pmatrix} + \begin{pmatrix} D_{11} & 0 \\ D_{21} & 0 \end{pmatrix} \left[\begin{pmatrix} D_{p11} \\ D_{p21} \end{pmatrix} (U_1) - \begin{pmatrix} h_1 \\ h_2 \end{pmatrix} \right] + \begin{pmatrix} Cr_{11} \\ Cr_{21} \end{pmatrix} (U_1) \\ \begin{pmatrix} \dot{h}_1 \\ \dot{h}_2 \end{pmatrix} = \begin{pmatrix} A_{11} \\ A_{21} \end{pmatrix} (\dot{U}_1) - \begin{pmatrix} B_{11} & 0 \\ B_{21} & 0 \end{pmatrix} \left[\begin{pmatrix} |\dot{U}_1| \\ 0 \end{pmatrix} \circ \begin{pmatrix} h_1 \\ h_2 \end{pmatrix} \right] \\ \qquad - \begin{pmatrix} \Gamma_{11} & 0 \\ \Gamma_{21} & 0 \end{pmatrix} \left[\begin{pmatrix} \dot{U}_1 \\ 0 \end{pmatrix} \circ \begin{pmatrix} |h_1| \\ |h_2| \end{pmatrix} \right] \end{cases} \tag{14}$$

For the piezotube which is a system with three inputs U_x, U_y and U_z and three outputs x, y and z ($n = k = 3$), the multivariable temperature-dependent model is:

$$\begin{cases} \begin{pmatrix} x \\ y \\ z \end{pmatrix} = \begin{pmatrix} \Gamma_{Tx} \\ \Gamma_{Ty} \\ \Gamma_{Tz} \end{pmatrix} + \begin{pmatrix} D_{xx} & D_{xy} & D_{xz} \\ D_{yx} & D_{yy} & D_{yz} \\ D_{zx} & D_{zy} & D_{zz} \end{pmatrix} \left[\begin{pmatrix} D_{pxx} & D_{pxy} & D_{pxz} \\ D_{pyx} & D_{pyy} & D_{pyz} \\ D_{pzx} & D_{pzy} & D_{pzz} \end{pmatrix} \begin{pmatrix} U_x \\ U_y \\ U_z \end{pmatrix} - \begin{pmatrix} h_x \\ h_y \\ h_z \end{pmatrix} \right] \\ \qquad + \begin{pmatrix} Cr_{xx} & Cr_{xy} & Cr_{xz} \\ Cr_{yx} & Cr_{yy} & Cr_{yz} \\ Cr_{zx} & Cr_{zy} & Cr_{zz} \end{pmatrix} \begin{pmatrix} U_x \\ U_y \\ U_z \end{pmatrix} \\ \begin{pmatrix} \dot{h}_x \\ \dot{h}_y \\ \dot{h}_z \end{pmatrix} = \begin{pmatrix} A_{xx} & A_{xy} & A_{xz} \\ A_{yx} & A_{yy} & A_{yz} \\ A_{zx} & A_{zy} & A_{zz} \end{pmatrix} \begin{pmatrix} \dot{U}_x \\ \dot{U}_y \\ \dot{U}_z \end{pmatrix} - \begin{pmatrix} B_{xx} & B_{xy} & B_{xz} \\ B_{yx} & B_{yy} & B_{yz} \\ B_{zx} & B_{zy} & B_{zz} \end{pmatrix} \left[\begin{pmatrix} |\dot{U}_x| \\ |\dot{U}_y| \\ |\dot{U}_z| \end{pmatrix} \circ \begin{pmatrix} h_x \\ h_y \\ h_z \end{pmatrix} \right] \\ \qquad - \begin{pmatrix} \Gamma_{xx} & \Gamma_{xy} & \Gamma_{xz} \\ \Gamma_{yx} & \Gamma_{yy} & \Gamma_{yz} \\ \Gamma_{zx} & \Gamma_{zy} & \Gamma_{zz} \end{pmatrix} \left[\begin{pmatrix} \dot{U}_x \\ \dot{U}_y \\ \dot{U}_z \end{pmatrix} \circ \begin{pmatrix} |h_x| \\ |h_y| \\ |h_z| \end{pmatrix} \right] \end{cases} \tag{15}$$

5. CONCLUSIONS AND PERSPECTIVES

This paper presented the characterization and the modeling of the temperature effect on the piezotube. The characterization has considered the direct transfers but also the cross-couplings between the piezotube axis. The sensitivity of the piezotube to the variation of the temperature (the thermo-mechanical gain) has been identified and compared to the electro-mechanical gain of the actuator, for X, Y and Z axis. The temperature-dependent model has been proposed and identified based on the characterization data of the X axis. The validation of this model proves its efficacy to model the temperature effect on piezoelectric actuators. The extension of this monovariable model to the multivariable modeling has also been proposed. Future works will concern the identification and the validation of the proposed multivariable model and the use of the temperature-dependent model for the design of the feedforward control laws of the temperature effect.

REFERENCES

[1] D. Santosh, E. Evangelos and S. O. R. Moheimani, "A survey of Control Issues in Nanopositioning", *IEEE Transactions on Control Systems Technology*, Vol. 15, pp. 802-823, 2007.

[2] A. J. Fleming, and K. K. Leang, "Design, Modeling and Control of Nanopositioning Systems", *Springer*, 2014.

[3] G. M. Clayton, S. Tien, K. K. Leang, Q. Zou, and D. Santosh, "A review of feedforward control approaches in nanopositioning for high-speed SPM", *J. Dyn. Syst., Meas., Control*, vol. 131, no. 6, pp. 061101-1061101-19, 2009.

[4] M. Rakotondrabe, I.A. Ivan, "Development and Force/Position Control of a New Hybrid Thermo-Piezoelectric MicroGripper Dedicated to Micromanipulation Tasks," *IEEE Trans. on Automation Science and Engineering*, vol.8, no.4, pp.824-834, Oct. 2011.

[5] R. Perez, J. Agnus, C. Clévy, A. Hubert, N. Chaillet, "Modeling, fabrication, and validation of a high-performance 2-DoF piezoactuator for micromanipulation," *IEEE/ASME Transactions on Mechatronics*, vol.10, no.2, pp.161-171, April 2005

[6] M. Rakotondrabe, I.A. Ivan, S. Khadraoui, C. Clévy, P. Lutz, N. Chaillet, "Dynamic displacement self-sensing and robust control of cantilever piezoelectric actuators dedicated for microassembly," *International Conference on Advanced Intelligent Mechatronics (AIM)*, pp.557-562, July 2010.

[7] X. Qingsong, "Precision Position/Force Interaction Control of a Piezoelectric Multimorph Microgripper for Microassembly," *IEEE Transactions on Automation Science and Engineering*, vol.10, no.3, pp.503-514, July 2013

[8] K. Rabenorosoa, C. Clévy, P. Lutz, A. N. Das, M. Rakesh, and D. Popa, "Precise motion control of a piezoelectric microgripper for microspectrometer assembly," *ASME International Design Engineering Technical Conferences and Computers and Information in Engineering Conference*, pp. 769-776, 2009.

[9] G. Binnig, and D. P. E. Smith, "Single-tube three-dimensional scanner for scanning tunneling microscopy", *Review of Scientific Instruments*, vol. 57, no. 8, pp. 1688-1689, 1986.

[10] M. Al Janaideh, P. Krejci, "Inverse Rate-Dependent PrandtlIshlinskii Model for Feedforward Compensation of Hysteresis in a Piezomicropositioning Actuator," *IEEE/ASME Transactions on Mechatronics*, vol. 18, no. 5, pp.1498-1507, 2013.

[11] K. K. Leang, D. Santosh, "Hysteresis, creep, and vibration compensation for piezoactuators: Feedback and feedforward control,", *Proceedings of the Second IFAC Conference on Mechatronic Systems*, 2002.

[12] D. Croft, G. Shed, D. Santosh, "Creep, hysteresis, and vibration compensation for piezoactuators: atomic force microscopy application," *Journal of Dynamic Systems, Measurement, and Control*, vol. 123, no. 1, p.p 35-43, 2001.

[13] M. Rakotondrabe, C. Clévy, P. Lutz. "Complete open loop control of hysteretic, creeped, and oscillating piezoelectric cantilevers", *IEEE Transactions on Automation Science and Engineering*, vol. 7, no. 3, p.p 440-450, 2010.

[14] A. J. Fleming, S. Aphale Sumeet, S. O. R. Moheimani, "A new method for robust damping and tracking control of scanning probe microscope positioning stages," *IEEE Transactions on Nanotechnology*, vol. 9, no. 4, p.p 438-448, 2010.

[15] D. Habineza, M. Rakotondrabe, Y. Le Gorrec, "BoucWen Modeling and Feedforward Control of Multivariable Hysteresis in Piezoelectric Systems: Application to a 3-DoF Piezotube Scanner," *IEEE Transactions on Control Systems Technology*, vol.23, no.5, pp.1797-1806, 2015.

[16] D. Habineza, M. Rakotondrabe, Y. Le Gorrec "Simultaneous Suppression of Badly-Damped Vibrations and Cross-couplings in a 2-DoF Piezoelectric Actuator, by using Feedforward Standard Hinf approach,"

Proc. SPIE, Next-Generation Robotics, vol. 94940, 2015.

[17] M. Rakotondrabe, "Modeling and compensation of multivariable creep in multi-DOF Piezoelectric Actuators", *IEEE International Conference on Robotics and Automation*, 2012.

[18] R. Khler, S. Rinderknecht,"A phenomenological approach to temperature dependent piezo stack actuator modeling", *Sensors and Actuators : Physica A*, vol. 200, p.p 123-132, 2013.

[19] M. Rakotondrabe, C. Clévy, P. Lutz. "Hinf deflection control of a unimorph piezoelectric cantilever under thermal disturbance," *IEEE/RSJ International Conference on Intelligent Robots and Systems*, 2007.

[20] A. Moure, A. Lemany, P. Ardo, "Temperature dependence of piezoelectric, elastic and dielectric coefficients at radial resonance of piezoceramics with an aurivillius-type structure," *IEEE Transactions on Ultrasonics, Ferroelectrics, and Frequency Control*, vol. 52, no. 4, p.p 570577, 2005.

[21] G. Martinet, F. Chatelet, A. Olivier, N. Hammoudi, S. Blivet, M. Fouaidy, H. Saugnac, "Low temperature properties of piezoelectric actuators used in SRF cavities cold tuning systems", *CARE-Conf-06-082-SRF*, 2006.

[22] R. Smith, F. Welsh, "Temperature dependence of the elastic, piezoelectric, and dielectric constants of lithium tantalate and lithium niobate", *Journal of applied physics* vol. 42, no. 6, p.p 22192230, 1971.

[23] M. Rakotondrabe, Y. Haddab, P. Lutz, "Quadrilateral Modelling and Robust Control of a Nonlinear Piezoelectric Cantilever," *IEEE Transactions on Control Systems Technology*, vol. 17, no. 3, pp.528-539, 2009.

[24] M. Rakotondrabe, "Dveloppement et commande modulaire dune station de microassemblage, "*PhD thesis*, *Université de Franche-Comté*, 2006.

[25] F. Preisach, "Ueber die magnetische Nachwirkung", *Zeitschrift fuer Physik*, vol. 94, pp. 277-302, 1935.

[26] L. Prandtl, "Ein Gedankenmodell zur kinetischen Theorie der festen Korper", *Z. Angew. Math. Mech.*, vol. 8, pp. 85-106, 1928.

[27] A. Y. Ishlinskii, "Some applications of statistical methods to describing deformations of bodies", *Izv. Akad. Nauk SSSR, Techn. Ser.*, Vol. 9, pp. 580-590, 1944.

[28] R. Bouc, "Forced vibration of mechanical systems with hysteresis", *Conference on Nonlinear Oscillation*, Prague, 1967.

[29] Y. K. Wen, "Method for random vibration of hysteresis systems", *Journal of the Engineering Mechanics Division*, vol. 102, pp. 249-263, 1976.

[30] L. Lennart, "System Identification Toolbox: For Use with Matlab. User's Guide. MathWorks Incorporated", 1995.